JOURNAL OF COMPUTATIONAL PHYSICS 69, 69–80 (1987)

Boundary Conditions at Outflow for a Problem with Transport and Diffusion

THOMAS M. HAGSTROM

Department of Applied Mathematics and Statistics, SUNY at Stony Brook, Stony Brook, New York 11794

Received August 30, 1985; revised May 23, 1986

We present a numerical test of a class of approximate boundary conditions at an artificial boundary for the solution of time-dependent problems in semi-infinite spatial domains. The conditions are constructed by use of a general method developed by the author in another work. A problem modeling the transport and diffusion of soluble matter by a parallel flow is taken as the test case. We demonstrate the effectiveness of the method in obtaining accurate results on small computational domains.

1. INTRODUCTION

An outstanding problem in the numerical solution of the partial differential equations of continuum mechanics is the proper treatment of artificial boundaries. A particular case of this is the problem of boundary conditions at an outflow boundary in fluid mechanics. In this work we present a numerical test of a general procedure for the derivation of boundary conditions for linear time-dependent problems.

Although many papers discussing boundary conditions for hyperbolic problems have appeared in the literature (see, e.g., Gustafsson and Kreiss [3] and Engquist and Majda [2]), much less has been written about parabolic problems. Hagstrom and Keller [6] present a method for nonlinear reaction–diffusion equations on the line. In that case, careful treatment of the "outflow" boundary conditions was shown to be crucial if the dynamics of wave propagation were to be simulated correctly.

In [4] the author has derived a class of asymptotic expansions for linear, time-dependent problems in cylindrical domains and used these expansions to construct a hierarchy of boundary conditions at an artificial boundary. Here, we apply this construction to the following problem:

$$\text{(a)} \quad \frac{\partial u}{\partial t} + a(y)\frac{\partial u}{\partial x} = D\left(\frac{\partial^2 u}{\partial x^2} + \frac{\partial^2 u}{\partial y^2}\right), \qquad x,\ t \geqslant 0,\ y \in (-1, 1),$$

$$\text{(b)} \quad u(0, y, t) = u_0(y, t),$$

0021-9991/87 $3.00

$$\text{(c)}\quad \frac{\partial u}{\partial y}(x, \pm 1, t) = 0,$$

$$\text{(d)}\quad \lim_{x \to \infty} u(x, y, t) = 0,$$

$$\text{(e)}\quad u(x, y, 0) = 0,$$

$$\text{(f)}\quad a(y) \geqslant 0. \tag{1.1}$$

Problem (1.1) is a model of the transport and diffusion of a scalar contaminant by a parallel flow whose profile is $a(y)$. For a theoretical and experimental discussion which is somewhat relevant to our work, the reader is referred to Taylor [8].

Beyond the inherent interest in its solution, we believe that (1.1) provides an excellent model problem to test our method on. First, it is relatively simple, yet the exact conditions at outflow are too complicated to use. Hence, our asymptotic approach is needed. Second, the effect of decreasing D, so that the equation becomes nearly hyperbolic, can be examined. Third, it has at least superficial similarities to the Navier–Stokes equations, which are an important motivation for our research.

In Sections 2 and 3 of this work the methods of [4] are applied to (1.1) to construct asymptotic expansions and boundary conditions. In Section 4 numerical results are given for a parabolic velocity profile. In particular, we assess the effects of the order of approximation to the boundary condition, the location of the artificial boundary and the value of the diffusion constant, D.

2. Asymptotic Expansion of the Normal Modes

Following [4] we seek a solution of (1.1) of the form:

$$\text{(a)}\quad u(x, y, t) = \sum_l u_l(x, y, t),$$

$$\text{(b)}\quad u_l(x, y, t) = \int_0^t c_l(p)\, Q_l(x, y, t-p)\, dp, \tag{2.1}$$

$$\text{(c)}\quad Q_l(x, y, t) = \frac{1}{2\pi i} \int_{-i\infty}^{i\infty} e^{st + \lambda_l(s)x} \cdot Y_l(y, s)\, ds.$$

This, in turn, leads to the eigenvalue problem,

$$\text{(a)}\quad sY_l(y, s) + \lambda_l a(y)\, Y_l(y, s) = D(Y_l''(y, s) + \lambda_l^2 Y_l(y, s)), \qquad y \in (-1, 1),$$
$$\text{(b)}\quad Y_l'(\pm 1, s) = 0. \tag{2.2}$$

We are particularly concerned with the behavior of u for large values of x and t. This leads us to the study of (2.2) for small values of s. Solutions can be expressed as a power series in s whose terms can be determined in order:

$$\begin{aligned} &\text{(a)} \quad Y_l(y, s) = Y_l^0(y) + sY_l^1(y) + \cdots, \\ &\text{(b)} \quad \lambda_l(s) = \lambda_l^0 + s\lambda_l^1 + s^2\lambda_l^2 + \cdots. \end{aligned} \tag{2.3}$$

The leading order eigenvalue–eigenfunction pair, $\{\lambda_l^0, Y_l^0\}$, is a solution of

$$\begin{aligned} &\text{(a)} \quad D(Y_l^{0\prime\prime} + (\lambda_l^0)^2 Y_l^0) - \lambda_l^0 a(y) Y_l^0 = 0, \qquad y \in (-1, 1), \\ &\text{(b)} \quad Y_l^{0\prime} = 0, \qquad y = \pm 1. \end{aligned} \tag{2.4}$$

Problem (2.4) can be solved numerically by a variety of methods (see, e.g., Keller [7]). As solutions of interest must be bounded as $x \to \infty$, we require that

$$\mathrm{Re}(\lambda_l^0) \leqslant 0. \tag{2.5}$$

Solutions of problems such as (2.4) have been used in the construction of asymptotic boundary conditions for steady problems (Gustafsson and Kreiss [3], Hagstrom and Keller [5], and Ache and Strikwerda [1]). In this particular case the solution with the smallest decay rate (in x) can be easily written down. It is

$$\begin{aligned} &\text{(a)} \quad \lambda_0^0 = 0, \\ &\text{(b)} \quad Y_0^0 = \text{constant} = 1. \end{aligned} \tag{2.6}$$

Formulas for Y_0^1, λ_0^1, and λ_0^2 are given in [4]. First, λ_0^1 is determined by the orthogonality condition,

$$\int_{-1}^{1} \{1 + \lambda_0^1 a(y)\}\, dy = 0, \tag{2.7}$$

which implies

$$\lambda_0^1 = \frac{-2}{[\int_{-1}^{1} a(y)\, dy]}. \tag{2.8}$$

The function $Y_0^1(y)$ is then a solution of:

$$\begin{aligned} &\text{(a)} \quad DY_0^{1\prime\prime} = 1 + \lambda_0^1 a(y), \qquad y \in (-1, 1), \\ &\text{(b)} \quad Y_0^{1\prime} = 0, \qquad y = \pm 1, \\ &\text{(c)} \quad \int_{-1}^{1} Y_0^1(y)\, dy = 0. \end{aligned} \tag{2.9}$$

Condition (2.9c) is necessary to make the solution unique.

Finally, λ_0^2 can be determined from another orthogonality condition

$$\int_{-1}^{1} \{ Y_0^1(y) + \lambda_0^2 a(y) + \lambda_0^1 a(y)\ Y_0^1(y) - D(\lambda_0^1)^2 \}\ dy = 0; \tag{2.10}$$

which implies

$$\lambda_0^2 = \frac{\int_{-1}^{1} \{ D(\lambda_0^1)^2 - (1 + \lambda_0^1 a(y))\ Y_0^1(y) \}\ dy}{[\int_{-1}^{1} a(y)\ dy]}. \tag{2.11}$$

For simple choices of $a(y)$, analytic expressions for these quantities can be found. In particular, if we choose a parabolic profile:

$$a(y) = (1 - y^2), \tag{2.12}$$

then

$$\begin{aligned} &\text{(a)} \quad \lambda_0^1 = -\tfrac{3}{2}, \\ &\text{(b)} \quad Y_0^1(y) = \frac{1}{120D}(15y^4 - 30y^2 + 7), \\ &\text{(c)} \quad \lambda_0^2 = \frac{27D}{8} + \frac{1}{35D}. \end{aligned} \tag{2.13}$$

An asymptotic expansion of $Q_l(x, y, t)$ for $|x| \gg 1$, $|\lambda_l^1 x + t|$, can be calculated by the method of descents (see [4]). A necessary condition for its validity is that $\lambda_l^{1,2}$ be real and

$$\lambda_l^1 \leqslant 0, \qquad \lambda_l^2 > 0. \tag{2.14}$$

We then have

$$Q_l(x, y, t) = e^{x[\lambda_l^0 - ((t + \lambda_l^1 x)^2/4\lambda_l^2 x^2)]} \cdot (Y_l^0(y)/\sqrt{4\pi\lambda_l^2 x}) \left(1 + O\left(\frac{(t + \lambda_l^1 x)^3}{x^2} + \frac{(t + \lambda_l^1 x)}{x}\right)\right). \tag{2.15}$$

The leading term of the expansion in (2.15) is closely related to a solution of the diffusion equation. If we assume that $\lambda_l^1 \neq 0$ and take

$$z = x + \frac{t}{\lambda_l^1}, \tag{2.16}$$

then (2.15) becomes

$$\begin{aligned} &\text{(a)} \quad Q_l(x, y, t) \sim e^{\lambda_l^0 x} F(z, t)\ Y_l^0(y), \\ &\text{(b)} \quad F(z, t) = e^{\{(\lambda_l^1)^3 z^2/4\lambda_l^2 t\}} \cdot (1/\sqrt{-4\pi\lambda_l^2 t/\lambda_l^1}). \end{aligned} \tag{2.17}$$

We see that F is an approximate solution of

$$\frac{\partial F}{\partial t} = \frac{-\lambda_l^2}{(\lambda_l^1)^3} \frac{\partial^2 F}{\partial z^2}. \tag{2.18}$$

Restating our results, we have found a basic solution of (1.1) which, far downstream, decays exponentially like a solution of the steady problem while translating at a certain speed and satisfying the effective diffusion law, (2.18). Note that (2.14), the necessary condition for the validity of the asymptotic expansion, guarantees that the effective diffusion constant will be nonnegative. For the parabolic profile, $a(y) = 1 - y^2$, this assumption is easily verified. We find that for $l = 0$ it is given by

$$D_{\text{eff}} = \frac{-\lambda_0^2}{(\lambda_0^1)^3} = D + \frac{8}{945D}. \tag{2.19}$$

This result was previously obtained by Taylor [8] using different methods and the value of D_{eff} was tested experimentally.

3. Construction of the Boundary Conditions

An exact boundary condition at $x = \tau$ is the relation between u and $\partial u/\partial x$ which, using (2.1), is implicitly given by

$$\begin{aligned} &\text{(a)} \quad \frac{\partial u}{\partial x}(\tau, y, t) = \sum_{\substack{l \\ \text{Re}(\lambda_l) > 0}} \frac{\partial u_l}{\partial x}(\tau, y, t), \\ &\text{(b)} \quad \frac{\partial u_l}{\partial x}(\tau, y, t) = \int_0^t c_l(p) \frac{\partial Q_l}{\partial x}(\tau, y, t-p)\, dp. \end{aligned} \tag{3.1}$$

Assuming that τ is large and that the most important contributions to the integral in (3.1) come from a neighborhood where $|\lambda_l^1 \tau + t - p| \ll \tau$, we use the expansions given above to approximate $\partial Q_l/\partial x$. In transform space we have

$$\frac{\partial \hat{Q}_l}{\partial x} = \lambda_l(s)\, \hat{Q}_l, \tag{3.2}$$

where $\lambda_l(s)$ is replaced by:

$$\lambda_l(s) = \lambda_l^0 + \lambda_l^1 s + \lambda_l^2 s^2 + \cdots. \tag{3.3}$$

Noting that s corresponds to $\partial/\partial t$ and taking derivatives outside the integrand we have a hierarchy of boundary conditions of increasing accuracy:

$$\text{(a)}\quad \frac{\partial u_l}{\partial x} - \lambda_l^0 u_l = 0,$$

$$\text{(b)}\quad \frac{\partial u_l}{\partial x} - \lambda_l^0 u_l - \lambda_l^1 \frac{\partial u_l}{\partial t} = 0, \tag{3.4}$$

$$\text{(c)}\quad \frac{\partial u_l}{\partial x} - \lambda_l^0 u - \lambda_l^1 \frac{\partial u_l}{\partial t} - \lambda_l^2 \frac{\partial^2 u_l}{\partial t^2} = 0.$$

Conditions (3.4a), (3.4b) are useful, but it is easily seen that (3.4c) leads to an ill-posed problem. This can be remedied by the trick of using Padé approximants (see Engquist and Majda [2]). That is, we replace (3.4c) by

$$\left(1 - \frac{\lambda_l^2}{\lambda_l^1}\frac{\partial}{\partial t}\right)\left(\frac{\partial}{\partial x} - \lambda_l^0\right) u_l = \lambda_l^1 \frac{\partial u_l}{\partial t}. \tag{3.4c'}$$

Higher order expansions could also be used.

The boundary conditions for all modes u_l could be included in a nonlocal condition on the channel cross-section [5]. However, given the exponential decay of the solutions, only the modes with the slowest decay are likely to be important. A one-mode condition is given by the application of (2.23) to u. Here we choose l so that λ_l^0 has the largest nonpositive real part. A two-mode condition can be calculated from the product of two one-mode conditions. For example, using (3.4c') for mode $l=0$ and (3.4b) for $l=1$ we have

$$\left(\frac{\partial}{\partial x} - \lambda_1^0 - \lambda_1^1 \frac{\partial}{\partial t}\right)\left(\frac{\partial}{\partial x} - \frac{\lambda_0^2}{\lambda_0^1}\frac{\partial^2}{\partial x\,\partial t} - \lambda_0^0 + \left[\lambda_0^0 \frac{\lambda_0^2}{\lambda_0^1} - \lambda_0^1\right]\frac{\partial}{\partial t}\right) u = 0. \tag{3.5}$$

In the computations we describe, at most two modes are considered.

4. Numerical Results

We now describe the results of numerical experiments. In all cases the parabolic profile is taken for $a(y)$ and periodic inflow forcing functions $u_0(y, t)$ are used. The results we show are only for

$$u_0(y, t) = 1 - \cos((1.0\bar{6})\,\pi t), \tag{4.1}$$

but are representative of the others. Outflow boundary locations of $\tau = 1, 3, 5$ are used and compared with results of a computation on a long interval ($\tau = 15$). One-mode boundary conditions (3.4a), (3.4b), (3.4c') based on the most slowly decaying

mode are tested as is the two-mode condition (3.5). For this the quantities λ_1^0 and λ_1^1 corresponding to the mode with the second slowest decay rate were computed:

$$\begin{aligned} &\text{(a)} \quad \lambda_1^0 = -1.351551109973, \\ &\text{(b)} \quad \lambda_1^1 = -0.3146578471274. \end{aligned} \tag{4.2}$$

The physical diffusion, D, is also varied. Results for $D = 1$ and 0.01 are given here.

The equations are discretized by the following two-step implicit splitting scheme

$$\begin{aligned} &(I - kD_{+x}D_{-x})(I - kD_{+y}D_{-y})\, u(x_i, y_j, t+k) \\ &\quad = 2ka(y_j)\, D_{0x} u(x_i, y_j, t) + (I + kD_{+x}D_{-x})(I + kD_{+y}D_{-y})\, u(x_i, y_j, t-k), \end{aligned} \tag{4.3}$$

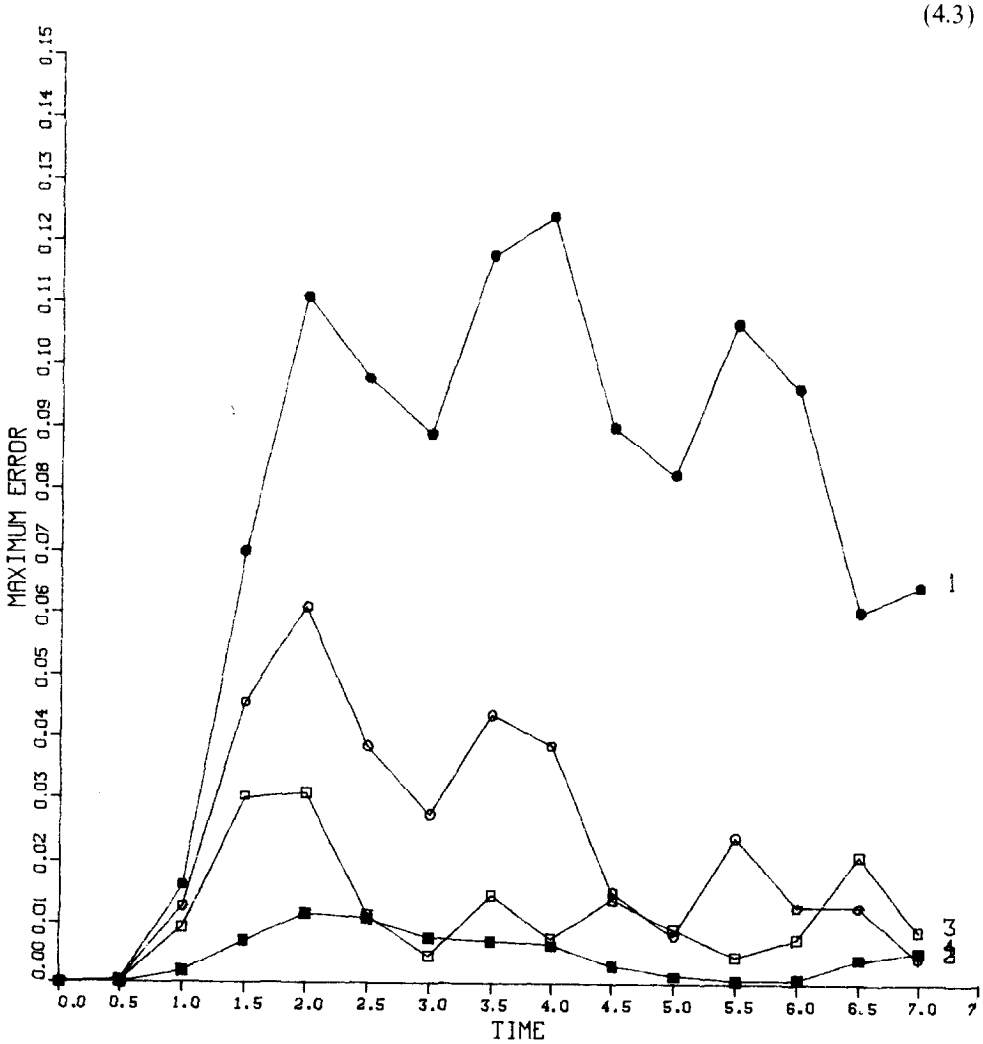

FIGURE 1.

where k is the time step and $D_{+,-,0}$ are standard spatial difference operators. The method is second order in space and time when used on uniform grids.

The one-mode boundary conditions, which involve only first order x derivatives, were implemented using centered differences across, at most, two mesh lines in x and t. In what follows we abbreviate $u(\tau, y_j, t)$ by $u^t_{\tau,j}$. Also, we use the symbols $A_{x,t}$ for averaging operators. That is:

$$\begin{aligned} &\text{(a)} \quad A_x u^t_{x,j} = \tfrac{1}{2}(u^t_{x+h,j} + u^t_{x,j}), \\ &\text{(b)} \quad A_t u^t_{x,j} = \tfrac{1}{2}(u^{t+k}_{x,j} + u^t_{x,j}). \end{aligned} \tag{4.4}$$

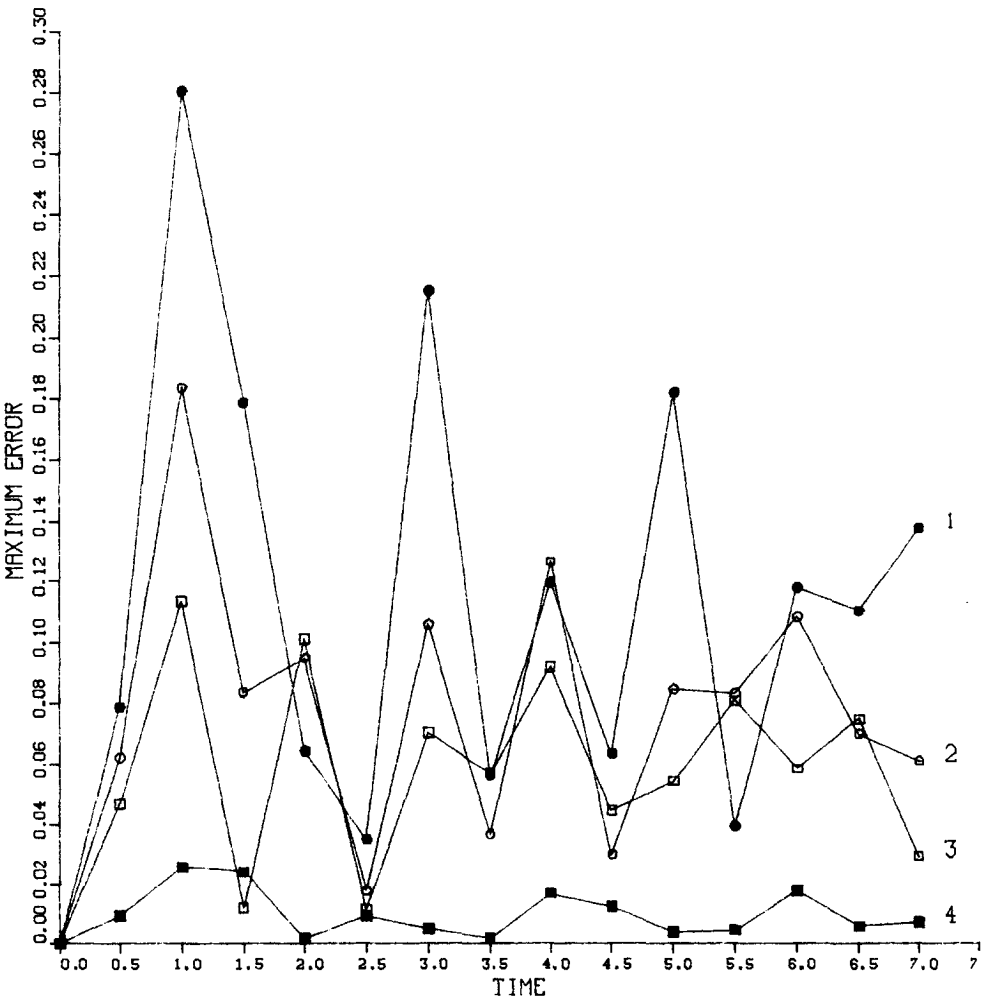

FIGURE 2.

We then have:

$$\text{(a)}\quad D_{+x}u_{\tau,j}^{t+k}-\lambda_0^0 A_x u_{\tau,j}^{t+k}=0,$$

$$\text{(b)}\quad A_t D_{+x}u_{\tau,j}^{t}-\lambda_0^0 A_t A_x u_{\tau,j}^{t}-\lambda_0^1 D_{+t}A_x u_{\tau,j}^{t}=0, \tag{4.5}$$

$$\text{(c)}\quad A_t D_{+x}u_{\tau,j}^{t}-\frac{\lambda_0^2}{\lambda_0^1}D_{+t}D_{+x}u_{\tau,j}^{t}-\lambda_0^0 A_t A_x u_{\tau,j}^{t}+\left(\lambda_0^0\frac{\lambda_0^2}{\lambda_0^1}-\lambda_0^1\right)D_{+t}A_x u_{\tau,j}^{t}=0.$$

Here, h is the mesh width in the x direction and, strictly speaking, the artificial boundary is located at $\tau+(h/2)$.

The implementation of (3.5), on the other hand, involves three mesh lines:

$$\left\{D_{+x}D_{-x}-\frac{\lambda_0^2}{\lambda_0^1}D_{+x}D_{-x}D_{0t}-(\lambda_0^0+\lambda_1^0)D_{0x}+\left(\lambda_0^1+\lambda_1^1-(\lambda_1^0+\lambda_0^0)\frac{\lambda_0^2}{\lambda_0^1}\right)D_{0x}D_{0t}\right.$$

$$\left.+\left(\lambda_0^0\lambda_1^1+\lambda_1^0\lambda_0^1-\lambda_0^0\lambda_1^0\frac{\lambda_0^2}{\lambda_0^1}\right)D_{0t}+\lambda_1^1\left(\lambda_0^1-\lambda_0^0\frac{\lambda_0^2}{\lambda_0^1}\right)D_{+t}D_{-t}+\lambda_1^0\lambda_0^0\right\}u_{\tau,j}^{t}=0. \tag{4.6}$$

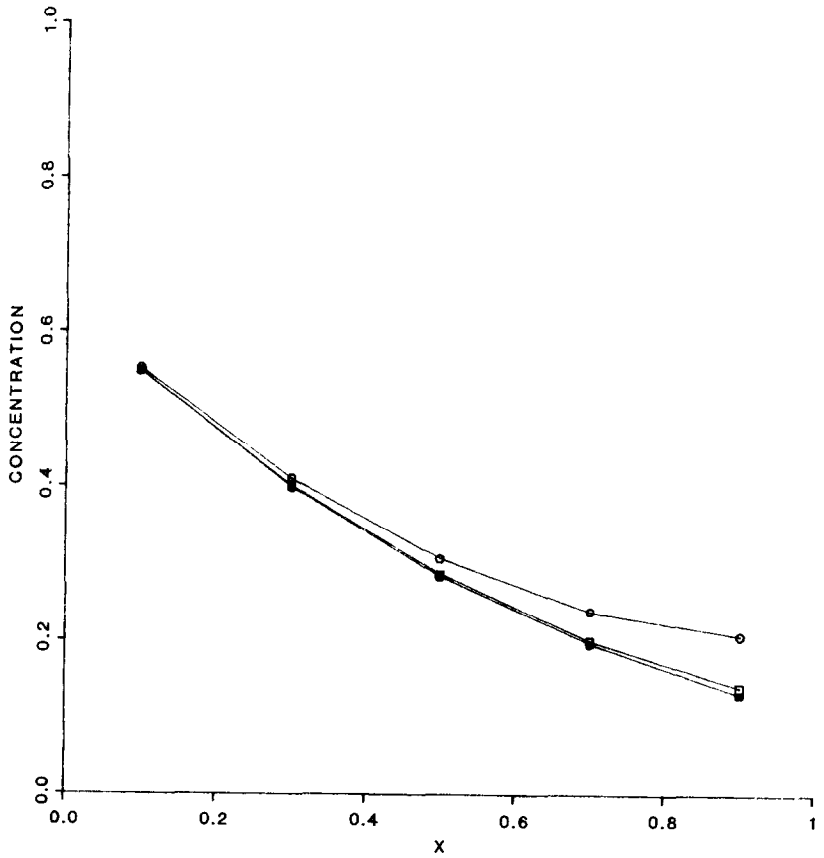

FIG. 3. (○), condition (4.5a); (□), condition (4.6); (●), long interval solution.

Figure 1 is a plot of the maximum error as a function of time and boundary condition for $\tau = 3$. Curves 1, 2, 3 correspond to (4.5a), (4.5b), (4.5c), respectively, while 4 corresponds to (4.6). The error is calculated from the assumption that the long interval solution is exact. The spatial mesh widths are both 0.1, the time step is 0.05 and $D = 1$. For short times we observe steady improvements as we progress from (4.5a)–(4.5c). For longer times there is, in this example, an improvement in the results using (4.5b). The two-mode condition (4.6) is seen to be consistently superior. This conclusion is more strongly supported by the results of taking $\tau = 1$, as depicted in Fig. 2. The success of the one-mode condition is significantly degraded, while that of (4.6) is not. A likely explanation is that, with τ so small, the exponential decay of the second mode has not yet drastically decreased the mode's amplitude. In fact, the results of using (4.6) with $\tau = 1$ appear to be better than those of (4.5) with $\tau = 3$. Figures 3–5 show snapshots of cross sections of the

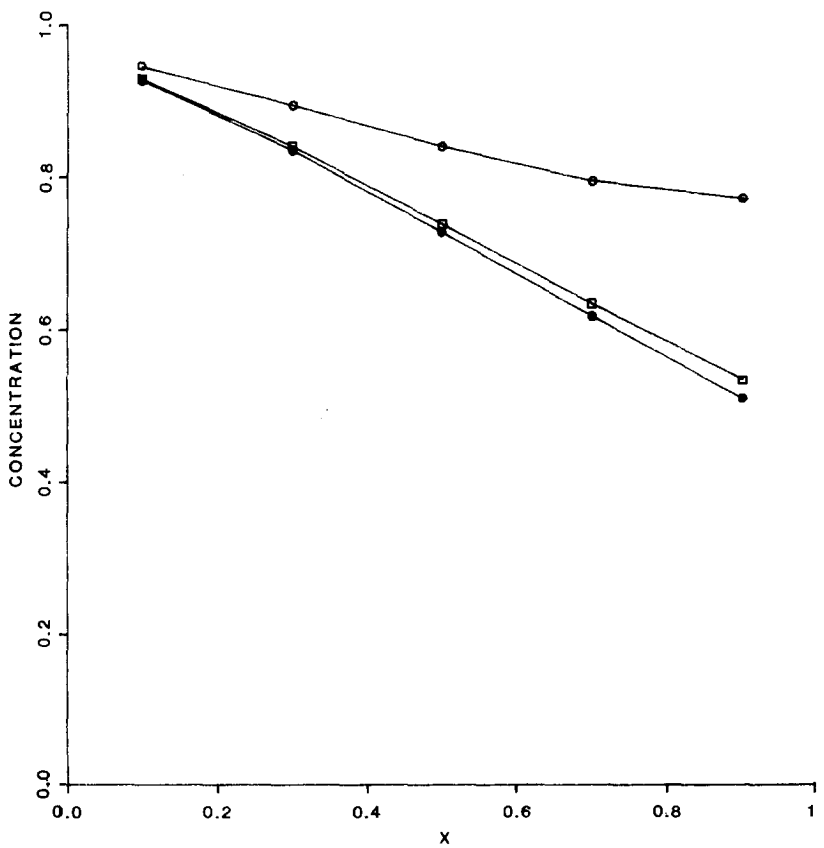

FIG. 4. See Fig. 3.

solutions on the short interval. For all of them $y = -0.05$. Depicted are the long interval solution ($\tau = 15$) along with those computed using (4.5a) and (4.6) with $\tau = 1$. A disturbance is seen to propagate through the boundary. As it does so, the results obtained using (4.5a) are seen to significantly deviate from the "exact" solution. Those obtained using (4.6), on the other hand, do not.

Finally, in Fig. 6, we plot the error for solutions satisfying (4.5a), (4.5b), (4.5c) with $D = 0.01$ and $\tau = 1$. The errors, in general, are lower than in the $D = 1$ case. Furthermore, the success of (4.5c) is degraded in comparison to that of (4.5b).

In conclusion, we have applied the method described in [4] to a simple problem and demonstrated its usefulness. At the price of solving an eigenvalue problem on the cross section, accurate results can be obtained with a significant decrease in the size of the computational domain.

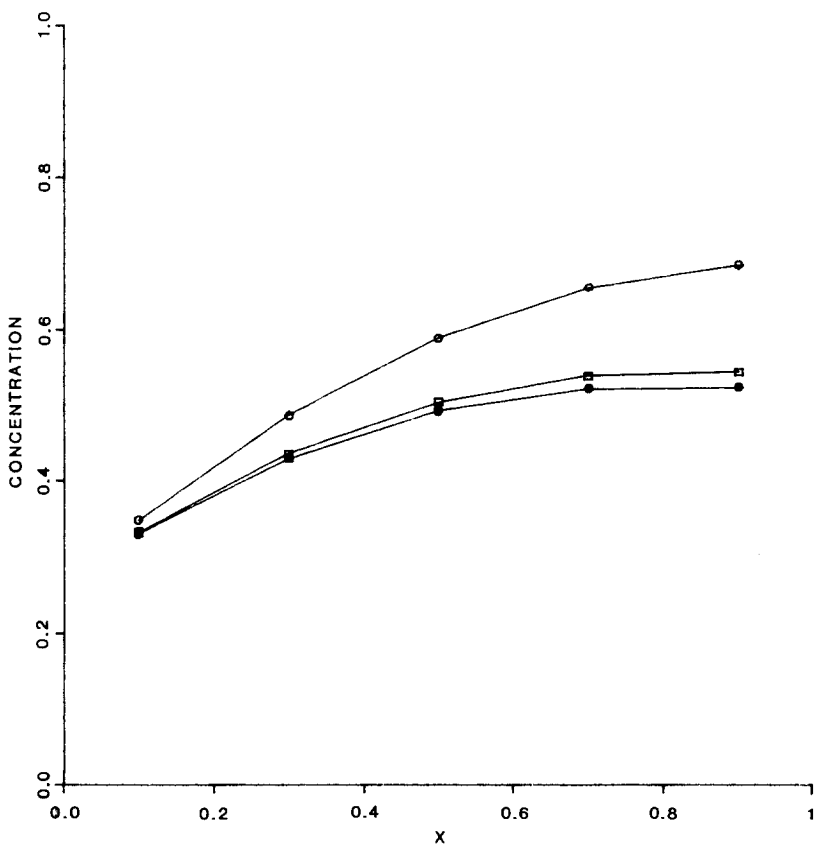

FIG. 5. See Fig. 3.

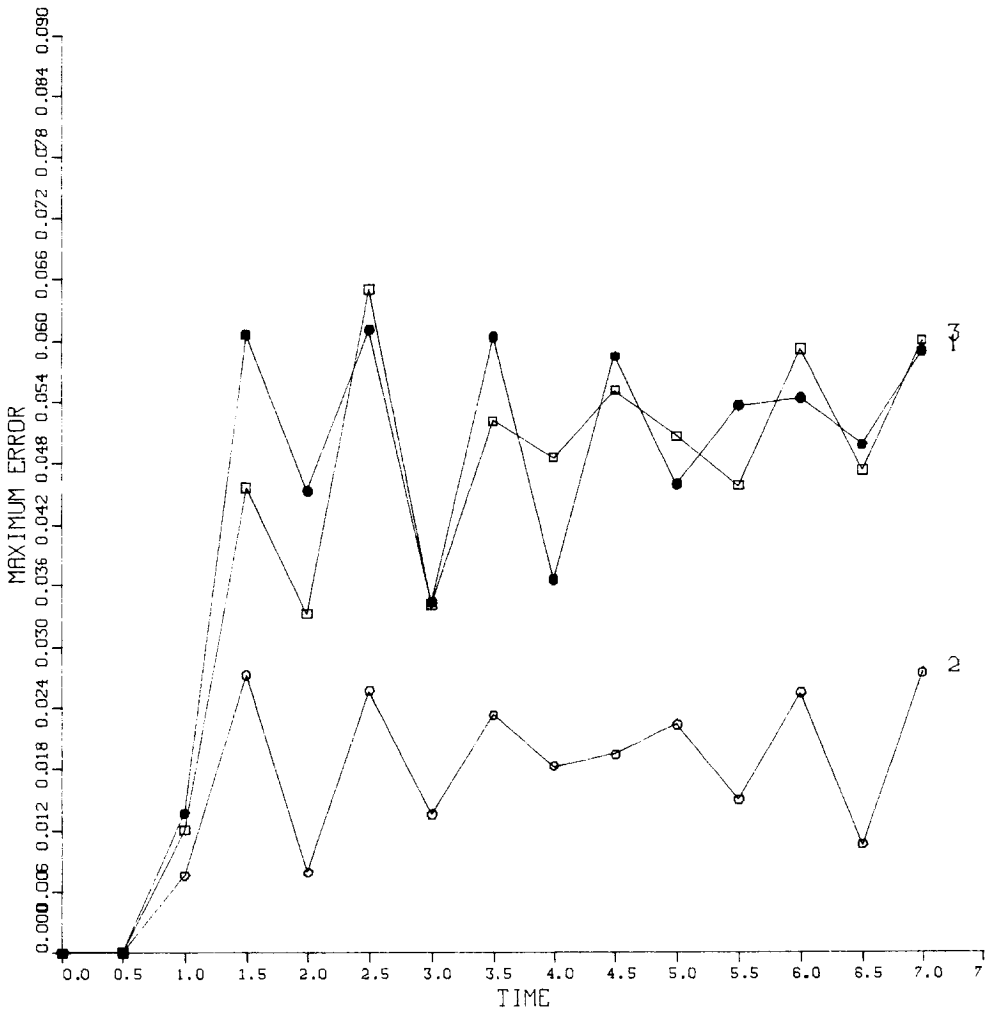

FIGURE 6.

ACKNOWLEDGMENTS

The author thanks the referees for their most useful suggestions.

REFERENCES

1. G. ACHE AND J. STRIKWERDA, to appear.
2. B. ENGQUIST AND A. MAJDA, *Math. Comput.* **31**, 139 (1977).
3. B. GUSTAFSSON AND H.-O. KREISS, *J. Comput. Phys.* **30**, 3 (1977).
4. T. HAGSTROM, *SIAM J. Numer. Anal.* **23**, 5 (1986).
5. T. HAGSTROM AND H. B. KELLER, *SIAM J. of Math. Anal.* **17**, 2 (1986).
6. T. HAGSTROM AND H. B. KELLER, *SIAM J. of Sci. Stat. Comput.* **7**, 3 (1986).
7. H. B. KELLER, "Numerical Solution of Two Point Boundary Value Problems," SIAM, Philadelphia (1976).
8. G. I. TAYLOR, *Proc. Roy. Soc. London Ser. A* **219**, 1137 (1953).